Exchange field on the rare earth Sm^{3+} in a single crystal perovskite SmMnO_{3}

J.-G. Cheng, J.-S. Zhou, J. B. Goodenough, Y. T. Su, Y. Sui, and Y. Ren

Phys. Rev. B **84**, 104415 — Published 8 September 2011

DOI: 10.1103/PhysRevB.84.104415

The exchange field on the rare earth Sm^{3+} in a single crystal perovskite $SmMnO_3$

J.-G. Cheng [1,2], J.-S. Zhou [1*], J. B. Goodenough [1], Y.T. Su [2], Y. Sui [2], and Y. Ren [3]

[1] Materials Science and Engineering Program/Mechanical Engineering, University of Texas at Austin, Austin, TX 78712, USA

[2] Center for Condensed Matter Science and Technology, Department of Physics, Harbin Institute of Technology, Harbin, 150001, China

[3] Advanced Photon Source, Argonne National Laboratory, Argonne, Illinois 60439, USA

Abstract

Single crystal $SmMnO_3$ has been grown by the floating-zone method. We have measured the magnetization and specific heat in magnetic fields oriented along three principal crystal axes of precisely oriented single crystals. Below T_N of the Mn^{3+}-ion array, the magnetic moments of the Sm^{3+} ions are progressively oriented antiparellel to the weak canted-spin ferromagnetic moment of the antiferromagnetic Mn^{3+}-ion array due to an internal exchange field $H_{in} \parallel c$. On cooling through a compensation temperature $T_{comp} \approx 9$ K, the dominant moment parallel to *c* changes from the canted-spin Mn^{3+} ions to the Sm^{3+} moments. A spin reversal in an $H_c \geq 1$ T changes the magnetic field splitting of the Kramers doublet on the Sm^{3+} ions from $H_{in} - H_c$ to $H_{in} + H_c$, where H_c is a field applied along the *c* axis. This change monitored by the Schottky contribution to the specific heat, creates an abrupt change at $T_t = T_{comp} \pm \delta$. We have found no evidence that the transition at T_t is first-order despite its abrupt nature.

I. Introduction

The perovskite manganites have received revived interest due to the discovery of the colossal magnetoresistance effect in mixed-valent $La_{1-x}A_xMnO_3$ (A = alkaline earth) [1, 2] and the recent observation of magnetoelectric effect (multiferroics) in the single-valent $RMnO_3$ (R = Gd, Tb, Dy).[3, 4, 5] With decreasing size of the rare-earth R^{3+} ion in single-valent $RMnO_3$, the type-A antiferromagnetic (AF) ordering on the Mn^{3+} -ion array for R = La – Sm changes to the type-E AF ordering for R = Ho – Lu. For the intermediate rare-earth ions R = Gd , Tb, and Dy, a sinusoidal AF ordering occurs where the long-wavelength magnetic ordering is accompanied by a lattice modulation via strong magnetoelastic coupling.[6] The evolution of magnetic structure as a function of the rare-earth ionic radius has been rationalized in terms of the change in the local structural distortions.[7] As seen from T_N of the Mn^{3+}-ion array versus the rare-earth radius over the entire phase diagram of perovskite $RMnO_3$, the influence of the magnetic rare earth on the spin ordering on Mn^{3+} appears to be negligible. However, the canted spins due to the type-A AF ordering on Mn^{3+} produce an exchange field at the rare-earth site, which not only leads to ordering magnetic moments on the rare earth ions at $T_{N'} < T_N$ but also creates different easy axes for the magnetic moment on the rare-earth site. Hemberger *et al.*[8] have carried out a comprehensive study on the magnetic and thermodynamic properties of $PrMnO_3$ and $NdMnO_3$ and revealed different anisotropic rare-earth contributions even though Pr^{3+} and Nd^{3+} have almost the same free-ion magnetic moments. A large saturation moment M_s of *ca.* 1.7 μ_B along the *c* axis was observed in $NdMnO_3$, which is about 20 times larger than those of $PrMnO_3$ and $LaMnO_3$ and cannot be accounted for by only the canted spins due to the type-A AF ordering from the Mn^{3+} sublattice. Instead, it has to be attributed to magnetic moments from Nd^{3+} polarized parallel to the weak ferromagnetic Mn3+-ion moment by Nd-Mn exchange coupling.[8] At low temperature, a 1.2(2) μ_B on Nd^{3+} coupled ferromagnetically has also been confirmed by neutron powder diffraction.[9] In contrast, the absence of a Pr^{3+}-ion moment along the *c* axis indicates that the Pr^{3+} moments are within the *ab* plane in $PrMnO_3$.[8]

Whereas the spin structure of $SmMnO_3$ from neutron diffraction is not available, magnetization measurements with the external field applied along different crystal axes

can help us to figure out how the rare-earth moment is ordered in the matrix of the ordered spins on Mn^{3+}. By applying a small magnetic field along the *c* axis, Mukhin *et al* [10] found a small increase of the magnetization M_c as it is cooled down through $T_N \approx 60$ K followed by a broad maximum at 30-40 K. The M(T) becomes negative as it is further cooled down below 9 K. The temperature for $M_c(T) = 0$ was labeled as a compensation temperature T_{comp}. The $M_c = 0$ at $T_{comp} \approx 9$ K can be interpreted by balancing the net ferromagnetic moment from the canted spins on Mn^{3+} by a moment from Sm^{3+} that is opposite. A recent report from Jung *et al* [11] has shown that the M(T) of $SmMnO_3$ actually depends on the magnitude of the magnetic field applied along the *c* axis. The M(T) no longer becomes negative at low temperatures for $H_c \geq 1$ T; instead, $M_c(T)$ exhibits an abrupt jump during cooling/warming at temperatures around T_{comp}. The spin-reversal transition also occurs in a sweeping magnetic field at a temperature below T_N. Jung *et al* have attributed the abrupt change of $M_c(T)$ to a reversal of the canted-spin moment and the moment on Sm^{3+} relative to the external field. Corresponding to the moment rotation, an abrupt change of magnetocapacitance was also observed. While the magnetic field-induced spin reversal transition has been verified by X-ray magnetic circular dichroism (XMCD) in the same report, whether it is first order and what causes the temperature-driven transition around T_{comp} under $H \geq 1$ T is not clear. In this paper, we report specific-heat measurements with magnetic fields applied on the three major crystallographic axes of a $SmMnO_3$ crystal. A Schottky-type contribution to C_p at low temperatures has been found in all cases. The energy gap Δ_g of the doublet ground state that contributes the Schottky-type anomaly in C_p, is sensitive to both the exchange and the external magnetic fields. The analysis of Δ_g versus H provides critical information for us to explain the temperature-driven transition found in M(T) and $C_p(T)$ as H is applied along the *c* axis.

II. Experimental details

The single-crystal $SmMnO_3$ used in this study was grown in an argon atmosphere from ceramic bars in an infrared-heating image furnace as described elsewhere.[12] The sample is single phase to powder X-ray diffraction. The oxygen stoichiometry has been checked carefully to within 0.1% by measurement of thermoelectric power as shown in Ref. 13. The Laue back reflection (LBR) was used to check the crystal quality and for the crystal

orientation. Sharp and uniform spots in LBR patterns of Fig.1 confirm the crystal quality; LBR patterns also show the precision of the crystal orientation. Measurements of the magnetization have been carried out in a Superconducting Quantum Interference Device (SQUID) magnetometer (Quantum Design). The specific heat was measured with a Physical Property Measurement System (PPMS-9T, Quantum Design) by using the two-τ relaxation method at temperatures from 2 to 100 K and under different magnetic fields up to 8 T. The background from the sample holder and the Apiezon N grease was recorded in a first run and was subtracted from the total specific heat. High-resolution synchrotron x-ray powder diffraction patterns at low temperatures and under magnetic fields were performed at the Advanced Photon Source (beamline 11-ID-C), Argonne National Laboratory.

III. Results and discussion.

Fig.2(a) shows the magnetization of $SmMnO_3$ crystal with H=0.05 T oriented along the principal crystal axes. The F_zA_y spin ordering of the Mn^{3+} array in the *Pbnm* crystal structure leads to a more dramatic increase of χ_c on cooling through T_N than that predicted from the Brillouin function for a regular ferromagnetic transition.[14] A crossover from dominance of the Mn^{3+}-ion canted spin ferromagnetism to dominance of the Sm^{3+}-ion magnetization on cooling through $T_{comp} \approx 9$ K causes the χ_c to exhibit a maximum at T ~ 35 K. The behavior of the low-field (H < 1 T) is consistent with that reported by Mukhin *et al.*[10] With atomic moments in the *b-c* plane, χ_a increases continuously below T_N because a perpendicular applied magnetic field $H_\perp$ cants the spins as in a Néel antiferromagnet; but χ_a is not constant below T_N because $SmMnO_3$ is ferromagnetic. What has not been reported is the $\chi_b(T)$; the FC $\chi_b(T)$ exhibits a minimum of T_{comp}. On cooling through T_N, the antiferromagnetic coupling of the Mn^{3+}-ion spins along the b axis progressively reduces $\chi_b(T)$ until the Sm^{3+}-ion moments dominate the canted-spin ferromagnetic moment below T_{comp}.

The magnetizations of Fig.2(b) for H parallel to the *a* and *b* axes are typical of an antiferromagnet. However, with H || *c* at 2K, $SmMnO_3$ shows a negative spontaneous magnetization along the *c*-axis even after cooling in zero field for a bar-shaped crystal

with long dimension along *c*. The magnetization loop of Fig.1(b) should be distinguished from that of a hard magnet by (1) an extremely sharp magnetization reversal at $H_{rev} = \pm 1$ T; (2) H_{rev} is significantly larger than the coercive force found in a ferromagnetic oxide; (3) the H_{rev} increases as temperature increases and peaks out at T_{comp}.[11] The unusual magnetization loop of Fig.2(b) has been interpreted to be the result of a spin reversal induced by H_c.[11]

The most unusual property is the butterfly-shape temperature dependence of the field-normalized magnetization M/H of Fig.3 for measurements during cooling and warming with magnetic fields $H_c \geq 1$ T. An abrupt change of the M/H has been found on cooling and warming at T_t and T_t' respectively, distributed symmetrically around T_{comp}. At $T < T_N$, the M/H becomes field dependent except at the temperature T_{comp} where all χ_c measured with different magnetic fields ($H \geq 1$ T) overlap precisely. The thermal hysteresis $\Delta T = T_t - T_t$' decreases as H increases; the ΔT versus H is illustrated in the insert of Fig.3. These abrupt changes are absent in $M_a(T)$ and $M_b(T)$. The abrupt transition of $M_c(T)/H$ around T_{comp} and the associated thermal hysteresis indicate the transition is possibly first order. However, the temperature dependence of the cell volume by synchrotron diffraction under H =5 T of Fig.4, which can discern a volume change as small as $\Delta V/V = 0.01\%$, shows no anomaly on crossing T_t. The refinement results for two temperatures around T_t listed in Table I reveal nearly identical Mn-O bond length and Mn-O-Mn bond angle on crossing T_t. In order to reveal the physics behind the temperature-driven transition in the magnetic susceptibility $\chi_c(T)$, we have performed measurements of specific heat C_p on $SmMnO_3$ crystals under a magnetic field to 8 T.

As shown in the insert of Fig.5, the C_p of $SmMnO_3$ exhibits a λ-shape anomaly at T_N similar to those found at T_N in other perovskite $RMnO_3$ (R = Pr, Nd).[8] The broad peak at $T < 5$ K has been observed in the $RMnO_3$ in which the ground state of the magnetic rare earth is a Kramers doublet or consists of two nearly degenerate states. The ground state of Sm^{3+} is a Kramers doublet, so the Schottky contribution to C_p and their field dependence can be found in measurements shown in Fig.5 regardless of the crystal orientation relative to the external field. Before getting into the detailed analysis of C_p, we can see easily that

applying a magnetic field moves the broad peak from the Schottky contribution to higher temperatures for H // a and H// b. However, if the field is applied on the *c* axis, it induces sharp changes in C_p at temperatures corresponding to transitions found in $\chi_c(T)$. The transition at T_t is not accompanied by a latent heat; no anomaly of the C_p has been found at T_t even with the temperature interval as small as the height of heat pulse ~ 0.3 K. We have also used the adiabatic method, *i.e.* monitoring the decay of a heat pulse that covers the transition temperature T_t. This method has been used successfully to pick up a latent heat associated with the extremely sharp first-order Verway transition in a Fe_3O_4 crystal. However, no latent heat can be resolved at the transition in $SmMnO_3$. A latent heat associated with the transition at T_t, if any, must be below the noise level of the C_p obtained by the adiabatic method. Taking the curve with H_c = 2 T for example, a minimum in C_p is fully developed for both cooling and warming curves. A high magnetic field appears to induce two distinct phases below and above T_t with a different field dependence of the Schottky contributions to C_p. This conjecture will be further verified by rigorous numerical analysis below.

The C_p of the $SmMnO_3$ crystal consists of three contributions, *e.g.* from the lattice and spin wave $C_{lat} + C_{sw}$, the Schottky contribution C_{Sch}, and the crystal field contribution C_{CF}. Both the $C_{lat} + C_{sw}$ and C_{CF} terms do not contribute to the low-temperature enhancement of C_p. We have used the $C_{lat} + C_{sw}$ obtained from the C_p of $LaMnO_3$ and the C_{CF} based on the crystal field splitting on Sm^{3+} in $SmNiO_3$.[15] The Schottky contribution is expressed as

$$C_{Sch} = R(\Delta_g / \kappa_B T)^2 \exp(\Delta_g / \kappa_B T) / [1 + \exp(\Delta_g / \kappa_B T)]^2 \qquad (1)$$

where Δ_g/κ_B is the splitting of the ground-state Kramers doublet or quasidoublet in the unit of temperature, κ_B is the Boltzmann constant, and R is the ideal gas constant. The doublet ground state of a free rare-earth ion is split in a crystal by the crystal field, the internal exchange field at the rare-earth site or an external magnetic field. Like the Mössbauer effect, the Schottky contribution C_{Sch} can be used as a local probe to study the exchange field in a magnetic crystal. The detailed field dependence of the gap for both Kramers doublet and quasidoublet can be found in ref.8. As shown in Fig.6(a), the C_p of $SmMnO_3$ is fit reasonably well with $C_{lat} + C_{sw} + C_{Sch} + C_{CF}$. The same procedure has been

carried out to fit C_p as the external magnetic field is applied along the *a* and *b* axes. The fitting results are shown in Fig.5(a,b) and the gap as a function of the external magnetic field is plotted in Fig.7. The most challenging problem is to identify why the C_p undergoes an abrupt change at T_t as H_c increases to above 1 T.

The enhancement in the low-temperature C_p due to the C_{Sch} creates a minimum around 10 K. For the C_p with H = 2 T, where the thermal hysteresis of the C_p associated with the transition is large, the two separate $C_p(T)$ curves of Fig.5(c) developed during warming and cooling have their minimum around 10 K. This important observation leads us to fit the C_p curves during cooling down and warming up with the same formula, but different energy gaps Δ_g of the Kramers doublet. As shown in Fig.6(b) where we have emphasized the low-temperature C_p mainly from the C_{Sch} , the fit works extremely well. The energy gap Δ_g for H_{ext} =0 is caused by the internal exchange field H_{in} at the Sm^{3+} site. We have plotted the field dependence of Δ_g in Fig.7; Δ_g decreases linearly as H_c increases for $T > T_t$, whereas it increases for $T < T_t$. The abrupt change of C_p at T_t is actually due to a transition between two states having opposite field-dependent gaps. The higher magnetic field, the larger difference between the energy gap Δ_g on crossing the transition. It is surprising that an abrupt change of C_p is accompanied by a tiny volume change that cannot be discerned by the high-resolution synchrotron diffraction. Although there is a large difference of the energy gap Δ_g on crossing the transition, the entropy change is so small that a latent heat $L = T\Delta S$ cannot be resolved by the C_p measurements in this work. The nature of the transition at T_t deserves further studies.

The C_p measurements under a magnetic field has been made previously on unoriented $NdMnO_3$ and $PrMnO_3$ crystals, which do not show the transition at low temperatures. The gap in both cases increases monotonically as H increases.[16, 17] In order to make a side-by-side comparison, we have performed the C_p measurements under a magnetic field on unoriented $SmMnO_3$ crystals. An abrupt change of C_p at T_t under a magnetic field has also been observed on the crystal in which the *c*-axis component of the external field appears to be larger than 1 T. Reduction of the doublet splitting under a magnetic field found in $SmMnO_3$ is a surprising result. This property and the abrupt change of C_p

around T_{comp} for H applied along the *c* axis must be related to the peculiar spin structure in perovskite $SmMnO_3$.

The spin canting due to either the single-ion anisotropic energy or the D-M antisymmetric exchange interaction in the type-A AF spin ordering creates a weak ferromagnetic moment along the *c* axis in the $RMnO_3$ perovskite with the *Pbnm* space group. The much more enhanced M_c at 5 K in $NdMnO_3$ indicates that the exchange field on the Nd site orders the Nd^{3+} moment parallel to the *c* axis and the Mn^{3+} canted-spin ferromagnetism. In $SmMnO_3$, however, the negative M_c below T_{comp} for $H_{ext} < 1$ T indicates the moment on Sm^{3+} is ordered antiparallel to the moment due to spin canting. This spin ordering configuration appears to be stable to the lowest temperature. The magnetization at 2 K changes sign from the virgin state as H increases to about 1 T as is shown in Fig.2(b). The magnetization changing sign is due to reversal of both the moment on Sm^{3+} and the canted spin ferromagnetism relative to the external field. The moment reversal also occurs as the crystal is cooled through $T_t < T_{comp}$. The canted spin moment is parallel to H_c at $T_{comp} < T < T_N$. Since the exchange field H_{in} on the Sm site is opposite to the canted spin moment and therefore the external field direction, the net field on the Sm site is $H_{in} - H_c$ in the temperature interval. The moment reversal below $T_t < T_{comp}$ places H_{in} in the same direction as H_c. The net field on the Sm site is $H_{in} + H_c$. Fig.7 indeed shows a linear dependence of Δ_g versus H_c. However, the magnitude of the $d\Delta_g/dH_c$ for $T > T_t$ is slightly higher than that for $T < T_t$, which reflects that the H_{in} is not a constant as H_c increases. As illustrated in Fig.7, the spin canting and therefore the $H_{in,}$ is reduced under H_c for $T < T_t$, whereas H_{in} increases slightly as H_c increases for $T > T_t$.

The same method in Fig.6(a) has been applied to fit the $C_p(T)$ data as the external magnetic field is applied on the a and b axes. Applying the external magnetic fields along *a* and *b* axes does not trigger the spin reversal. The external field H_{ext} is orthogonal to the H_{in}. In these cases, the energy gap in C_{Sch} is proportional to $[(\mu H_{in})^2 + (\mu H_{ext})^2]^{1/2}$, which is consistent with the non-linear dependence of Δ_g versus H_c observed.

IV. Conclusion

The exchange field on the rare earth Sm^{3+} in perovskite $SmMnO_3$ places the rare-earth moment antiparallel to the canted spin moment from Mn^{3+}. While the external field on the *c* axis strengthens the canted-spin moment and therefore the exchange field in the interval $T_t < T < T_N$, competition for lowering the energy of the rare-earth moment in the external field leads to a reversal of the *c*-axis components of the spins at $T < T_t$. This transition has been assumed in the literature to be first-order. Our crystal-structure study under a high magnetic field indicates no abrupt volume change on crossing the transition temperature within the resolution $\Delta V/V \approx 0.01\%$ of the synchrotron diffraction used in this work. Furthermore, a latent heat associated with the transition, if any, cannot be resolved by our specific-heat measurements under a magnetic field. The ground state of Sm^{3+} is a Kramers doublet. By studying the Schottky contribution to the low-temperature specific heat in different magnetic fields, we have demonstrated that the abrupt change of C_p at T_t is caused by a transition between two states having opposite field-dependent energy gaps splitting the Sm^{3+} Kramers doublet.

Acknowledgements

This work was supported by NSF (DMR 0904282) and the Robert A Welch foundation (Grant F-1066). The Advanced Photon Source is supported by the U. S. Department of Energy Office of Science, under Contract No. DE-AC02-06CH11357.

* jszhou@mail.utexas.edu

Table 1 Results of the Rietveld refinements to the high-resolution synchrotron XRD patterns of $SmMnO_3$ under H = 5 T below and above T_t.

$SmMnO_3$, H = 5T	T =15 K	T =5 K
a (Å)	5.4309(3)	5.4311(3)
b (Å)	5.9079(4)	5.9083(4)
c (Å)	7.5476(5)	7.5474(5)
V ($Å^3$)	242.17(3)	242.18(3)
Mn-O1(Å)	1.955(2)	1.955(2)
Mn-$O2_1$ (Å)	2.244(6)	2.249(7)
Mn-$O2_2$ (Å)	1.946(6)	1.950(7)
<Mn-O> (Å)	2.0482(2)	2.051(3)
<Sm-O> (Å)	2.502(2)	2.495(3)
Mn-O1-Mn (°)	149.67(8)	149.65(9)
Mn-O2-Mn (°)	146.5(3)	145.7(3)
R_p (%)	3.91	3.82
R_{wp} (%)	4.35	4.16
χ^2 (%)	0.517	0.456

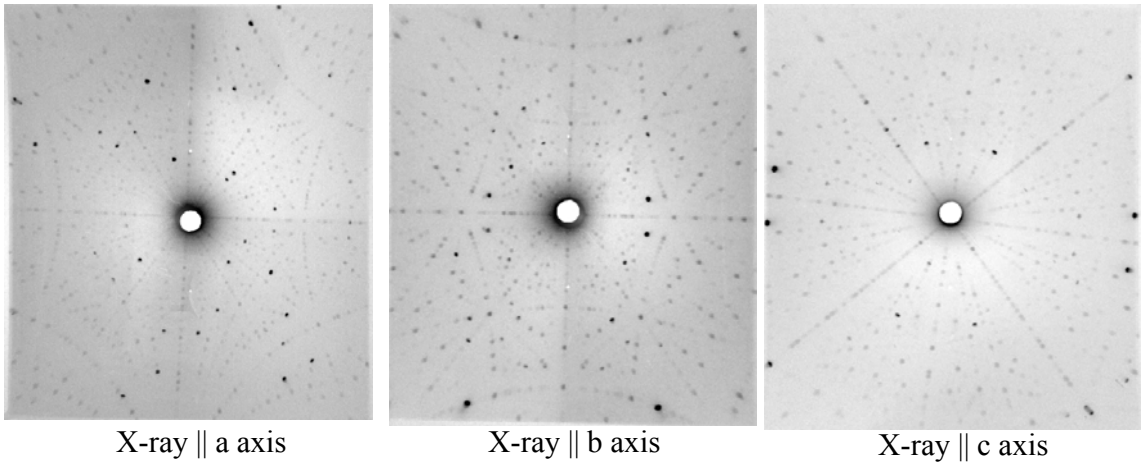

Fig.1 Laue back reflection of $SmMnO_3$ crystals for X-ray beam along three principal axes.

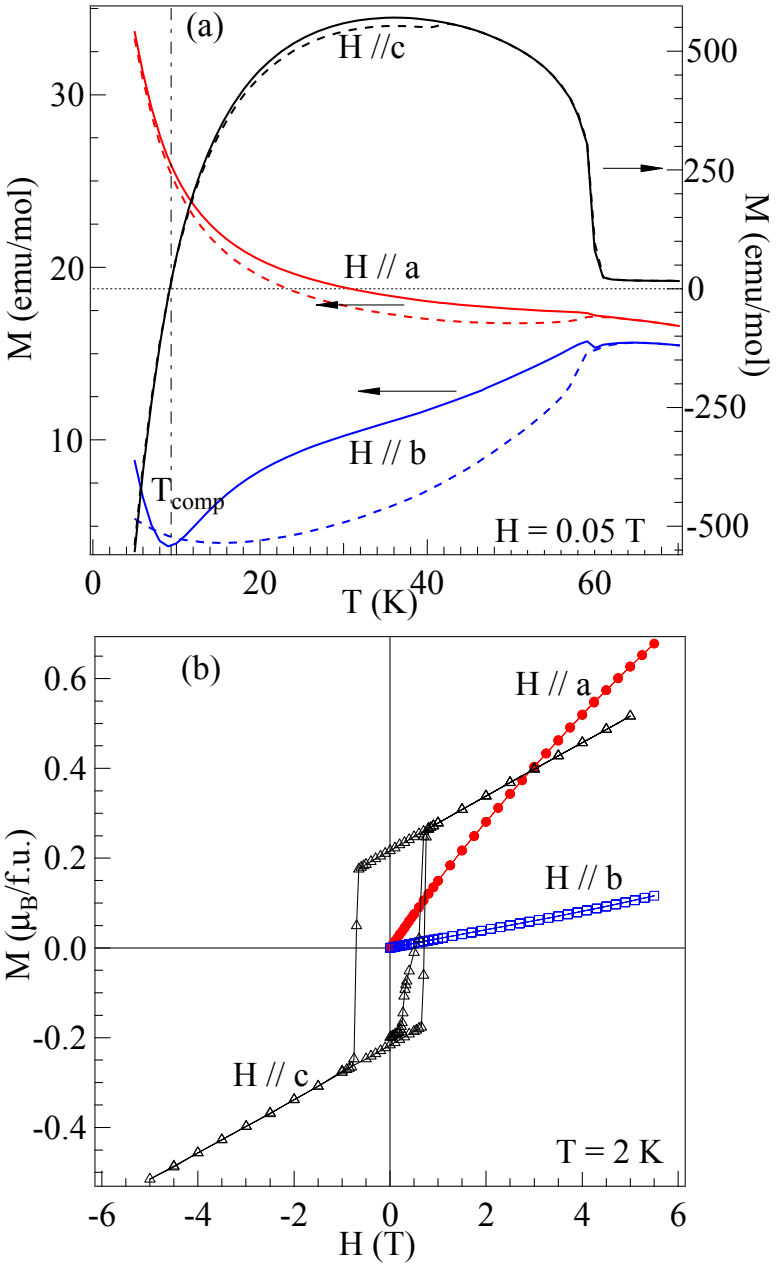

Fig.2 (Color online) (a) Temperature dependence of the magnetization; solid lines for field cooled and dashed lines for zero-field-cooled; (b) the magnetization for the single crystal $SmMnO_3$ at T = 2 K with magnetic field applied along all three major crystallographic axes.

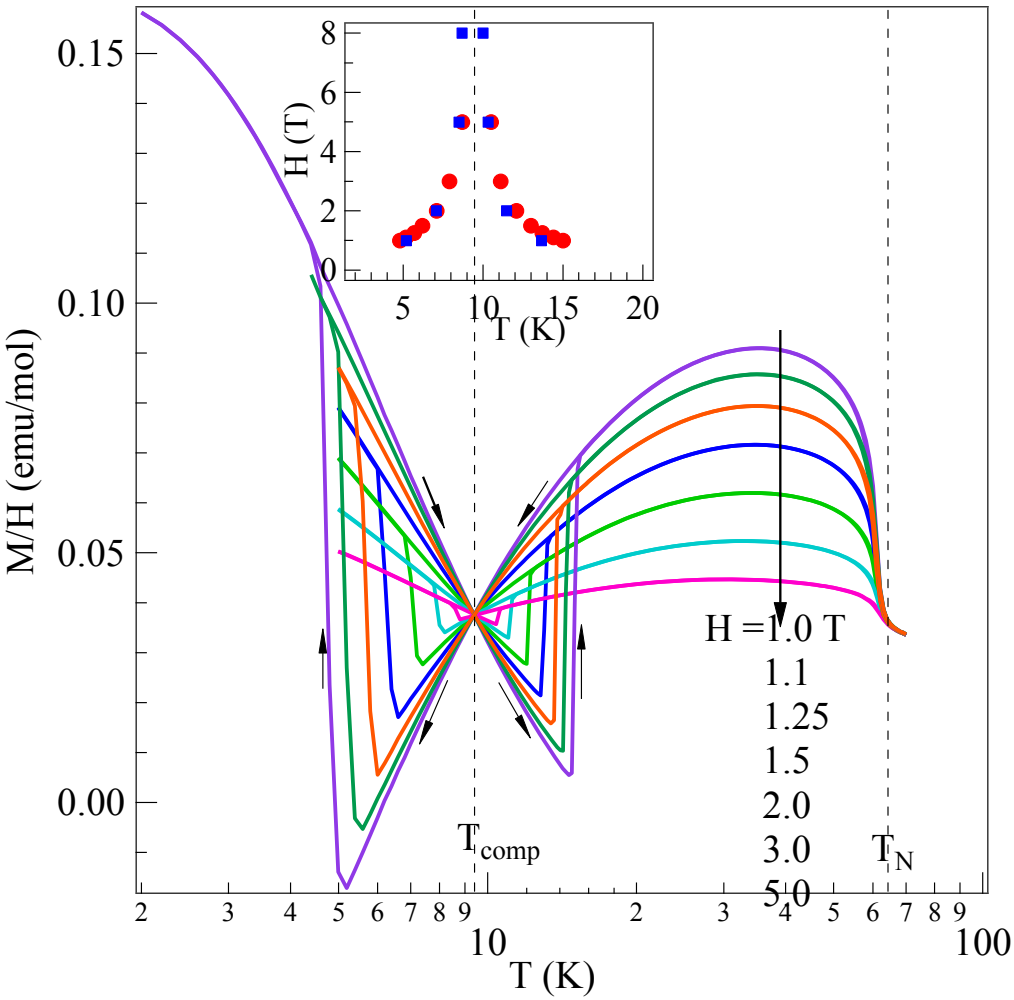

Fig.3 (Color online) Temperature dependence of M/H for the $SmMnO_3$ crystal with magnetic field applied along the *c* axis. Since the magnetization of the $SmMnO_3$ crystal with magnetic field applied along the *c* axis in Fig.2(b) does not go through origin, M/H used in this plot does not represent the normal magnetic susceptibility. The insert plot shows transition temperature T_t and T_t' found for different magnetic fields.

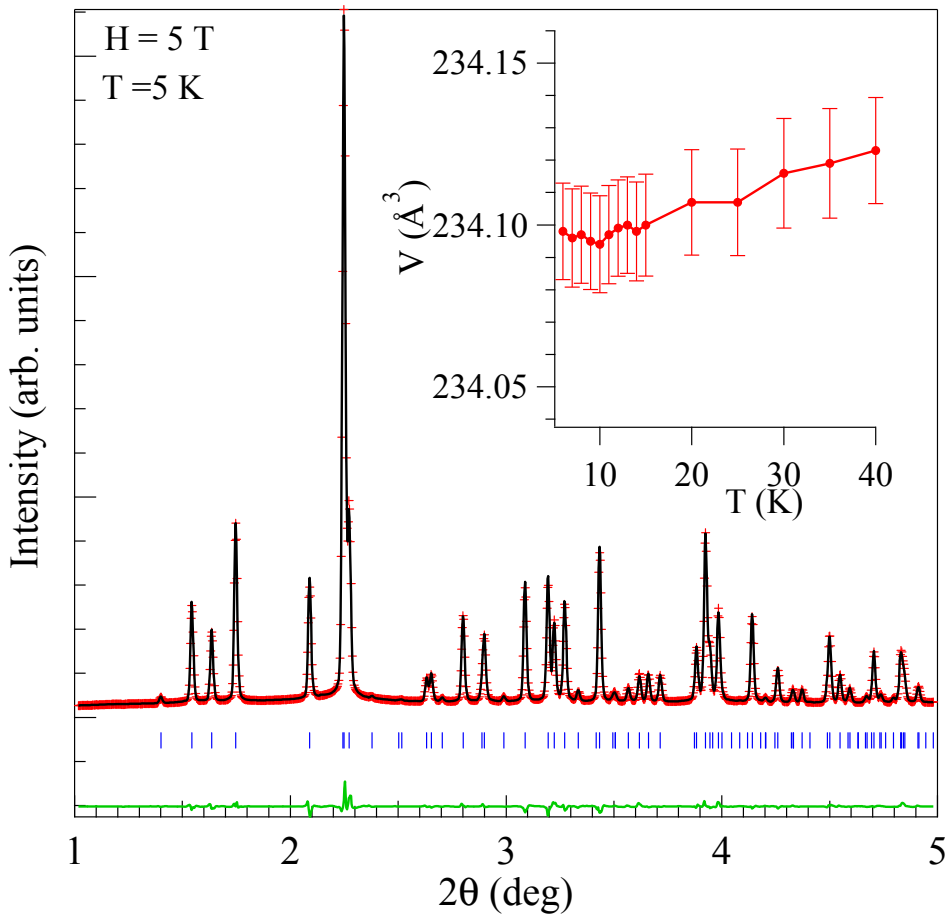

Fig. 4 (Color online) High-resolution synchrotron X-ray diffraction patterns of $SmMnO_3$ with the wavelength $\lambda = 0.10775$ Å under a magnetic field H = 5 T; the inset shows the temperature dependence of the cell volume.

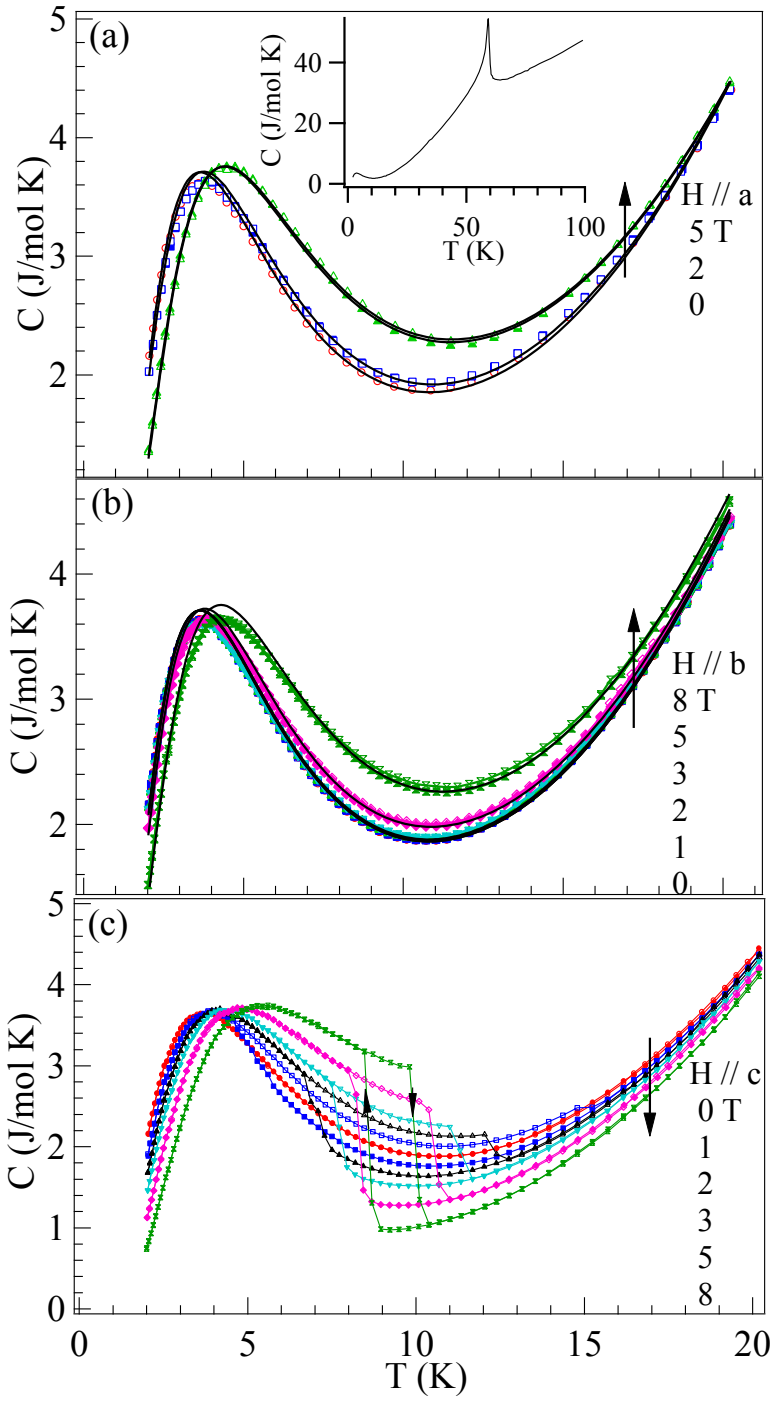

Fig.5 (Color online) Temperature dependence of specific heat C_p for the $SmMnO_3$ crystal with different magnetic fields applied along the three major crystallographic axes; the insert shows the C_p for a broader temperature range.

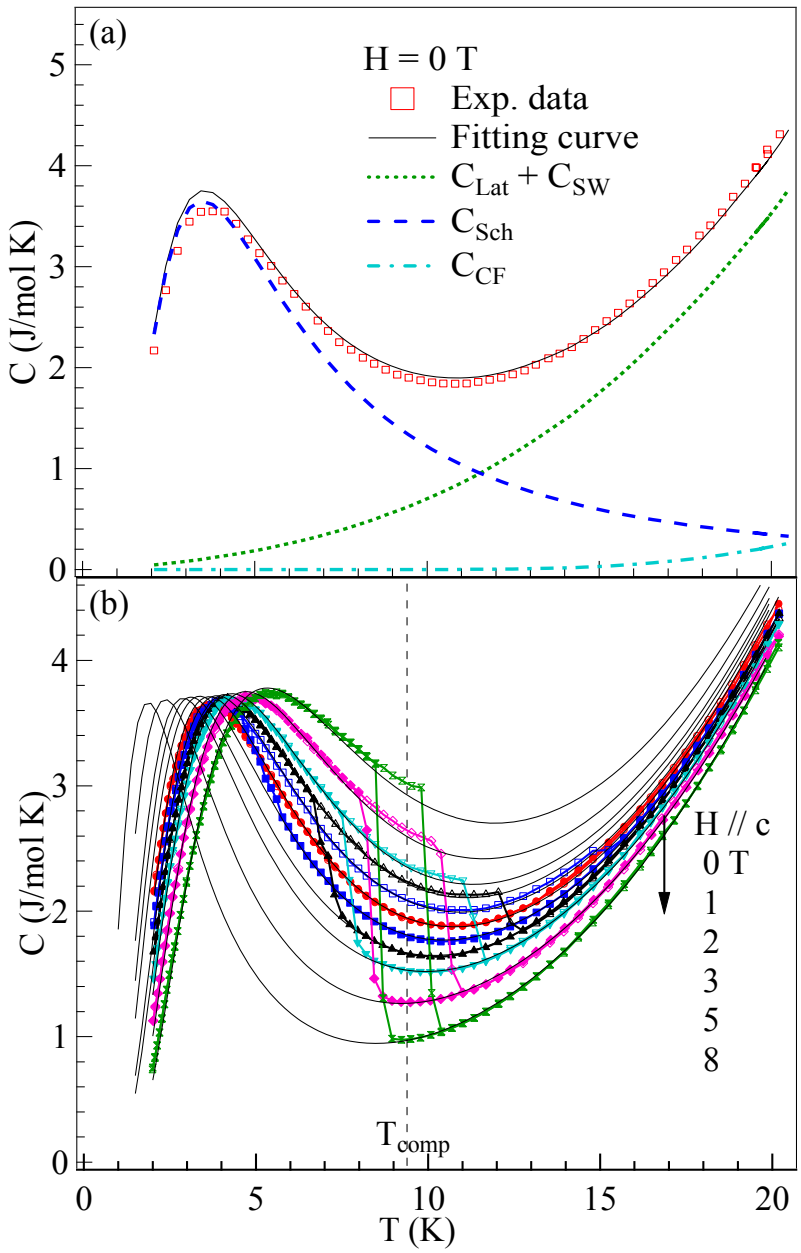

Fig.6 (Color online) Temperature dependence of C_p for the $SmMnO_3$ crystal. (a) The final fitting curve for H=0 is decomposed into three contributions; (b) The detailed fitting results for the C_p curves during cooling and warming by the curve shown in (a), but with different splitting Δ_g of the Kramers doublet.

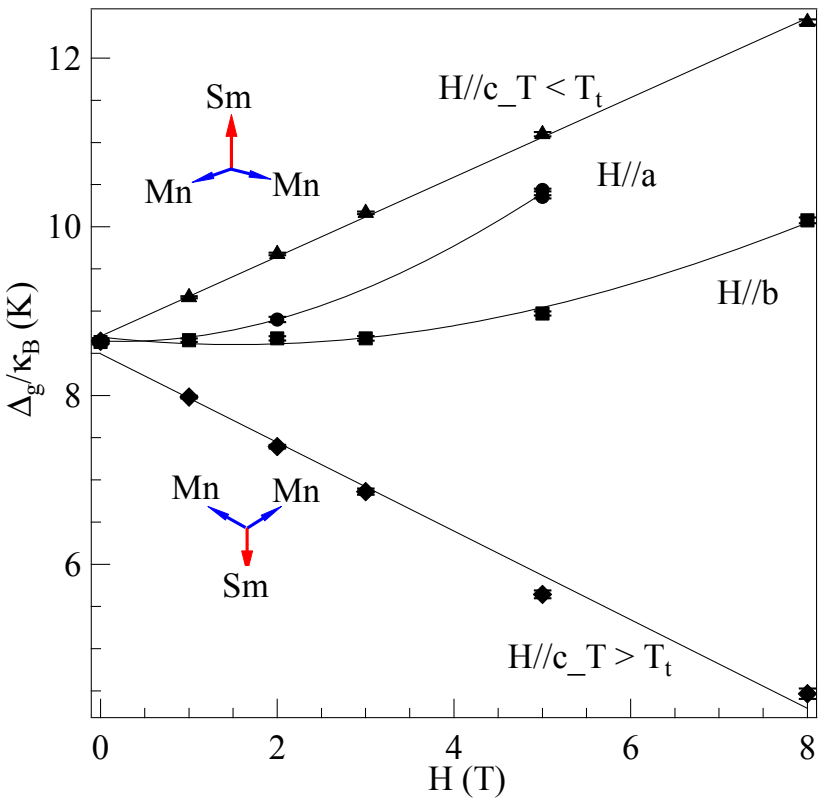

Fig.7 (Color online) The magnetic field dependence of the energy gap Δ_g obtained as the external magnetic fields are applied along different crystal axes. The size of error bar is nearly the same as that of symbols used in the plot. The insert illustrates the moments of canted spin from Mn^{3+} and Sm^{3+}.

---

[1] R. von Helmolt, J. Wecker, B. Holzapfel, L. Schultz, and K. Samwer, Phys. Rev. Lett. **71**, 2331 (1993).

[2] S. Jin, T. H. Tiefel, M. McCormack, R. A. Fastnacht, R. Ramesh, and L. H. Chen, Science **264**, 413 (1994).

[3] T. Kimura, T. Goto, H. Shintani, K. Ishizaka, T. Arima, and Y. Tokura, Nature **426**, 55 (2003).

[4] T. Goto, T. Kimura, G. Lawes, A. P. Ramirez, and Y. Tokura, Phys. Rev. Lett. **92**, 257201 (2004).

[5] T. Kimura, G. Lawes, T. Goto, Y. Tokura, and A. P. Ramirez, Phys. Rev. B **71**, 224425 (2005).

[6] T. Kimura, S. Ishihara, H. Shintani, T. Arima, K. T. Takahashi, K. Ishizaka, and Y. Tokura, Phys. Rev. B **68**, 060403(R) (2003).

[7] J.-S. Zhou and J. B. Goodenough, Phys. Rev. Lett. **96**, 247202 (2006).

[8] J. Hemberger, M. Brando, R. Wehn, V. Yu Ivanov, A. A. Mukhin, A. M. Boabashov, and A. Loidl, Phys. Rev. B **69**, 064418 (2004).

[9] A. Muñoz, J. A. Alonso, M. J. Martínez-Lope, J. L. García-Muñoz, and M. T. Fernández-Díaz, J. Phys.: Condens. Matter **12**, 1361 (2000).

[10] A. A. Mukhin, V. Yu Ivanov, V. D. Travkin, A. S. Prokhorov, A. M. Balbashov, J. Hemberger, and A. Loidl, J. Mag. and Mag. Mater. **272-276**, 96 (2004).

[11] J.-S. Jung, A. Iyama, H. Nakamura, M. Mizumaki, N. Kawamura, Y. Wakabayashi, and T. Kimura, Phys. Rev. B **82**, 212403 (2010).

[12] J.-S. Zhou and J. B. Goodenough, Phys. Rev. B **68**, 144406 (2003).

[13] J.-S. Zhou and J. B. Goodenough, Phys. Rev. B **68**, 054403 (2003).

[14] T. Moriya, in *Magnetism*, edited by G. T. Rado and H. Suhl (AP, NY, 1963), Vol. **I**, p.86.

[15] S. Rosenkranz, M. Medarde, F. Fauth, J. Mesot, M. Zolliker, A. Furrer, U. Staub, P. Lacorre, R. Osborn, R. S. Eccleston, and V. Trounov, Phys. Rev. B **60**, 14857 (1999).

[16] J.-G. Cheng, Y. Sui, Z. N. Qian, Z. G. Liu, J. P. Miao, X. Q. Huang, Z. Lu, Y. Li, X. J. Wang, and W. H. Su, Solid State Commun. **134**, 381 (2005).

[17] J.-G. Cheng, Y. Sui, X. J. Wang, Z. G. Liu, J. P. Miao, X. Q. Huang, Z. Lu, Z. N. Qian, and W. H. Su, J. Phys.: Condens. Matter **17**, 5869 (2005).